

IL-10/STAT3 signalling pathway-mediated T-cell suppressors upregulation in severe HFMD with EV71 infection

Yaozhong Zhang

Dongguan Institute of Pediatrics

Qi Peng

Dongguan Institute of Pediatrics

Xu Yuan

Dongguan Institute of Pediatrics

Zitian Lin

Dongguan Institute of Pediatrics

Zaixue Jiang

Dongguan Institute of Pediatrics

Yinghong Zhang

Dongguan Children's Hospital Affiliated to Guangdong Medical University

Xing Guo

Dongguan Children's Hospital Affiliated to Guangdong Medical University

Xiaomei Lu

Dongguan Institute of Pediatrics

Baimao Zhong (✉ zbm@dgp-institute.com)

Dongguan Children's Hospital Affiliated to Guangdong Medical University

Article

Keywords: Enterovirus 71, Arg-1, iNOS, COX-2, IL-10/STAT3 signalling, HFMD

Posted Date: June 14th, 2022

DOI: <https://doi.org/10.21203/rs.3.rs-1714168/v1>

License:   This work is licensed under a Creative Commons Attribution 4.0 International License.

[Read Full License](#)

Abstract

Enterovirus 71 (EV71) causes outbreaks of hand, foot and mouth disease (HFMD) in many countries, especially in the Asia-Pacific region. The EV71 engages diverse strategies to escape immune responses during infections. Arg-1, iNOS and COX-2 are particular suppressors secreted by MDSCs to inactivate T cells, which have been considered to play a significant role in the immune escape of viruses or malignant tumours. However, whether EV71 escapes the immune response through T-cell suppressors remains unknown. We established an animal model of HFMD by EV71 infection in BALB/c mice. The expressions of cytokines IL-10 and Arg-1, iNOS and COX-2 were detected by ELISA and qRT-PCR. The phosphorylation of STAT3 was detected by western blot. The number of MDSCs in PBMCs was examined by flow cytometry. The number of MDSCs in HFMD mice was significantly higher than that in the control, which is in agreement with the upregulation of T-cell suppressors (Arg-1, iNOS and COX-2) secreted by MDSCs in the infection group. The percentage of the gMDSC subpopulation was significantly increased in severe HFMD mice. The serum level of IL-10 and p-STAT3 were upregulated significantly in the infected group whilst inhibition of IL-10 and STAT3 led to the reduction in the T-cell suppressors. Our results suggest that T-cell suppressors (Arg-1, iNOS and COX-2) upregulated in HFMD in response to EV71 infection is attributable to STAT3 signalling activation triggered by IL-10 induction. We speculate that it was caused by elevation of MDSCs to facilitate the immune escape of EV71 in severe HFMD.

Introduction

Hand, foot and mouth disease (HFMD) is a worldwide public health problem with high infection rates in children under five years old, particularly in the Asia-Pacific region [1–3]. Enterovirus 71 (EV71) is the main cause of severe manifestations of the disease. EV71 infection may result in aseptic encephalitis, pulmonary oedema, circulatory disorders and even death, and seriously threatens the life and health of infants and young children [4, 5]. To date, the pathogenesis of severe HFMD remains unclear, and the key to reducing the mortality from this disease is to clarify the pathogenesis and to determine surveillance markers for the early identification effective targeted therapy.

Upon EV71 infection, several alterations in innate and adaptive immunity occur including the activation of STAT3 signalling pathway and the release of numerous host cytokines and proinflammatory factors, such as COX-2 and iNOS [6–9]. COX-2 and iNOS are particular suppressors secreted by MDSCs to inactivate T cells, facilitating viral escape and disease development [10–12]. MDSCs first found in tumour patients and Dutch rat tumours in the late 1970s [13], are a heterogeneous population of immature cells derived from myeloid progenitors with immune-suppressive functions [14]. They are present in low numbers in the peripheral blood of healthy individuals and rapidly expand during pathological conditions, including cancer, autoimmune or infectious diseases, trauma, sepsis and bone marrow transplantation, in response to the acute and excessive inflammatory conditions [15–17]. Recent studies have shown that MDSCs in infectious diseases interact with pathogenic microorganisms, emphasizing their key role in the immune escape of the virus and replication [18–20].

In this study, we found a positively correlation among the level of Arg-1, iNOS, COX-2 and the number of MDSCs and the degree of HFMD symptoms. We further confirmed that the IL-10-mediated STAT3 activation is attributable to the upregulation of Arg-1, iNOS, COX-2 and dysfunctional T cells help to facilitate immune escape of EV71, and the upregulation of T-cell suppressors might be caused by expansion of MDSCs. Our study provides new insights into the pathogenesis of severe HFMD and may help to develop novel strategy in the disease management.

Materials And Methods

Ethic statement

All procedures were approved by the Animal Ethics Committee of Guangdong Medical University, in accordance with the relevant guidelines and regulations on Animal Care. All animal experiments were performed in accordance with the ARRIVE guidelines (Animal Research: Reporting of In Vivo Experiments). Balb/C mice were fed with aseptic fodder and water and kept in IVC (individual ventilated cages) which maintained sanitary and cosy environment the for SPF (specific pathogen free) animals. We also made utmost efforts to minimize sufferings of animals during experiments.

Virus amplification

EV71 was augmented in Vero cells. We used the 50% tissue culture infectious dose (TCID₅₀) assay with the Reed-Muench method to determine and calculate the virulence of viruses cultured in Vero cells. To gain an effective and infective mouse strain, we domesticated EV71 by intraperitoneally injecting BALB/c mice with the strain and then recycled the virus by extracting the supernatant of thigh tissue grinding fluid from infected mice. Finally, we repeated this procedure until the mice became infected with EV71 and showed evident symptoms of severe HFMD.

Experimental animal treatment

To establish the EV71-infected severe HFMD model, 100 μ L of 1×10^6 TCID₅₀ of EV71 was intraperitoneally injected for 2 consecutive days and diluted with RPMI 1640 culture medium; in addition, the control group was treated with the same volume of medium. 3 or 4 days later, some model mice had severe symptoms of HFMD, including respiratory failure, quadriplegia and weight loss; another group of mice injected with the virus showed mild symptoms of tetraplegia and weight loss. The standards for severe and mild symptoms were previously published [21,22, 23]. Infected mice were divided into a severe group (respiratory failure, quadriplegia and weight loss) and a mild group (tetraplegia and weight loss), according to the observed symptoms.

Histopathological examination

We stripped skeletal muscle from the thigh of the mouse and then immediately fixed the tissue with 10% neutral buffered formalin. The tissues were embedded in paraffin, sectioned, and stained with

haematoxylin and eosin or incubated with the EV71 antibody; then, the samples were histopathologically examined. The morphology suggested that the BALB/c mice with severe HFMD caused by EV71 was established successfully and could be used for subsequent experimental procedures.

Flow cytometry

Cells were isolated and suspended in 4°C PBS (phosphate-buffered saline) with 2% heat-inactivated foetal bovine serum and 2 mM EDTA. Antibodies against CD11b, Ly-6G, and Ly-6C were purchased from BD Biosciences. Cells were analysed using a flow cytometer (FACSVerse, BD Biosciences). The data were analysed with FlowJo software (TreeStar, Inc.).

ELISA

The expression levels of Arg-1, iNOS, COX-2, IL-2, IL-4, IL-6, IL-10, and TNF- α in serum were detected with an ELISA kit (CUSABIO) on the basis of the manufacturer's specifications. The absorbance of the samples in 96-well plates was read at 450 nm by an automated microplate reader (BioTek).

Western blot

Western blot assay was carried out as follow: cells were lysed with RIPA buffer and cleared lysate was collected by centrifugation for protein separation on 10% SDS- polyacrylamide gel. The proteins were transferred onto PVDF membranes (Millipore) and detected with respective antibodies at 4°C overnight, Immunoblot analysis was performed with the ECL-chemiluminescence kit in accordance with manufacturer's protocol. Primary antibodies against STAT3 (Abcam), p-STAT3 (Abcam) and GAPDH (Proteintech) were used.

Primary PBMC extraction and culture

PBMCs were obtained from the whole blood of healthy BALB/c mice at 6-8 weeks of age, and we used Ficoll separation to gather PBMCs from the whole blood of mice, according to the manufacturer's instructions. The primary cells were cultivated at 37°C in a CO2 incubator.

Cell viability assay

The T cells (2×10^4 /well) were seeded in 96-well plates in a total volume of 200 μ l for 24h, and then were infected with EV71 at different doses TCID₅₀ for 24 to 96h. We investigated the effect of EV71 infection on the viability of T cells using a CCK8 assay kit (Beyotime).

Quantitative PCR

We extracted total RNA from tissues and primary cells with TRIzol reagent (DP405, Tiangen) and then synthesized the cDNA by reverse transcribing total RNA to single-stranded RNA using a reverse transcription system (B24408, BioMake). Then, qPCR was performed using 2 \times SYBR Green qPCR Master Mix (B21203, BioMake) with an Applied Biosystems StepOnePlus Real-Time PCR System, according to

the manufacturer's specifications. Primers were designed to detect the expression levels of target genes (Table 1). A separate analysis using primers for the detection of RPL35A was used as an internal control.

Statistical Analysis

The distribution of variables was determined by normal Q-Q plots. Research data are shown as the means \pm SEM. The statistical significance of the differences between groups was determined by one-way ANOVA using the program SPSS 13.0. Correlations between variables were calculated using the Spearman rank-order correlation. All P values were two-sided. P values less than 0.05 were considered statistically significant in all cases.

Results

Study subjects

The immunohistochemistry examination and qRT-PCR results showed higher number of EV71 copies in the severe symptoms group compared to those in the mild symptoms and control groups (Fig. 1a). Furthermore, the histopathological examination revealed that the samples in the severe symptoms group exhibited more inflammatory cell infiltration and serious damage in tissues, including striated muscle rupture, rhabdomyolysis in the muscle on the femur, more alveolar oedema and congestion in the lung (Fig. 1b). The level of CK in the serum showed the same trend as the results above (Fig. 1c). All the data and images indicated that the disease model with EV71 infection could develop different symptoms of the same disease.

Correlations between MDSCs and EV71 in HFMD

In total, twenty-three EV71-infected mice and 10 control mice were enrolled in the study. MDSCs were defined as either CD11b⁺ and Ly-6G⁺ cells (gMDSCs), or CD11b⁺ and Ly-6C⁺ cells (mMDSCs) (Fig. 2a). The percentage of gMDSCs in mice with severe symptoms (n=12) was significantly higher than those in mice with mild symptoms (n=11) and in the control mice (n=10) (p<0.05). Nevertheless, the mMDSC percentage showed no significant differences among these groups (P>0.05) (Fig. 2b).

The expression of T-cell suppressors and cytokines in different groups

MDSCs have the ability to hinder immune responses in diverse ways in different cancers or infectious diseases by secreting some suppressors to disturb the T-cell response. Therefore, we collected the serum of peripheral blood from mice in each group and then detected the expression of the most remarkable T-cell suppressors secreted by MDSCs and other cytokines, including IL-4, IL-6, IL-10, and TNF- α ; The results revealed that the highest expression of suppressors were found in the severe symptoms group; furthermore, the level of IL-10 positively correlated to the severity of the disease. Therefore, increased IL-10 expression during EV71 infection may result in the expansion of gMDSCs which in turn leads to the upregulation of Arg-1, iNOS, COX-2 (Fig. 3).

EV71 facilitates the inhibitory effects on T cells through the IL-10/STAT3 signalling pathway

To gain further insight into the influence of IL-10 on the expression of T-cell suppressors, we verified the STAT3 activation in EV71-treated PBMCs. Our data showed that there was no dose-dependent correlation between either T-cell suppressors or IL-10 and the concentration of EV71. The intensity of inhibitory effect of gMDSCs did not correlate with the viral concentration (Fig. 4a). The addition of S31-201, an inhibitor of p-STAT3, remarkably blocked the STAT3 phosphorylation triggered by EV71 and IL-10, suggesting that EV71 infection induces IL-10 to regulate the phosphorylation of STAT3 (Fig. 4b). Moreover, qPCR results showed that similar to EV71 infection, addition of IL-10 also induced significant increase in Arg-1, COX-2, and iNOS. On the other hand, the STAT3-specific inhibitor S31-201 dramatically decreased the levels of Arg-1, COX-2, and iNOS in EV71-treated PBMCs (Fig. 4c), the immunohistochemistry examination results showed higher number of T-cells infiltration in the mild symptoms group compared to those in the severe symptoms (Fig. 4d), further confirming that the IL-10/STAT3 signalling pathway mediates the immune response in EV71 infection triggered HFMD.

Discussion

MDSCs have been shown to be significantly increased in malignancies, autoimmune diseases, and viral infectious diseases [24–26]. Arg-1, COX-2, and iNOS are typical T cell suppressors secreted by MDSCs [27–29]. Furthermore, different MDSC subsets with various phenotypic and functional features are classified as granulocytic MDSCs (gMDSCs) and monocytic MDSCs (mMDSCs)[30]. Accumulating evidence indicates that gMDSCs play a vital role in regulating the immune environment [31–33].

Recent reports have shown that the upregulation of Arg-1, COX-2, and iNOS may facilitate and maintain the persistent HCV or HBV infection [34–36]. However, the association between the upregulation of Arg-1, COX-2, iNOS and EV71 infection in HFMD, have not been elucidated. Our results showed that upon EV71 infection, there is dosage dependent increase in gMDSCs. In addition, both the T-cell suppressors (Arg-1, iNOS and COX-2) and IL-10 were upregulated in HFMD. Previous studies have suggested that the percentage of gMDSCs likely correlates with the pathological symptoms, level of cytokines such as IL-6, IL-10, TNF- α and TNF- γ , and the expression of viral structural protein, or tumor stage [37–39]. Our research indicated that gMDSCs is positively correlated with the level of IL-10, pathological symptoms and viral replication.

It has also been reported that IL-10 and IL-12 were associated with inflammation progress during viral infection [40, 41]. However, it is unclear if there is a correlation between IL-10 and T-cell suppressors (Arg-1, iNOS and COX-2) during EV71 infection. EV71 infection significantly increased the release of circulating IL-10, the production of IL-10 was increased with disease clinical stage[42]. In this study, we confirmed that EV71 infection promote the expression of T-cell suppressors by upregulating IL-10. Previous study showed that transcription factor STAT3 can be activated through binding of IL-10 to its cognate receptor on MDSCs [43, 44]. In this study, we revealed that T-cell suppressors-mediated immune suppression in HFMD is mediated through STAT3 signaling in an IL-10-dependent manner.

However, how EV71 triggers the upregulation of the IL-10 and how STAT3 signaling promotes MDSCs expansion remain unclear. Elucidating the mechanism behind will provide fundamental knowledge on the pathogenesis of severe HFMD.

In conclusion, our study revealed that EV71 infection promotes the IL-10/STAT3-dependent upregulation of T-cell suppressors (Arg-1, iNOS and COX-2), which in turn results in the impaired T-cell function, leading to a severe HFMD. Our data suggested that the immune escape of EV71 is likely due to the expansion in MDSCs which results in increased T-cell suppressors, eventually leading to T cells dysfunction.

Declarations

Funding

The study was supported by the Key Projects of Science and Technology Plan of Dongguan (Project Number: 2017507150100444, 20185071501001618 and 2019507150100185); Guangdong Medical Research Fund Project (Project Number: B2019044). The funders had no role in the design of the study or in the collection, analysis and interpretation of data or in writing the manuscript.

Conflict of interest

The authors declare no conflict of interest.

Data Availability Statement

Related data are available from the corresponding author upon reasonable request.

References

1. Puenpa Jiratchaya, Wanlapakorn Nasamon, Vongpunsawad Sompong, Poovorawan Yong (2019). The History of Enterovirus A71 Outbreaks and Molecular Epidemiology in the Asia-Pacific Region. *J Biomed Sci*, 26(1), 75. doi:10.1186 /s12929-019-0573-2.
2. Qiu Jun, Yan Haipeng, Cheng Nianci, Lu Xiulan, Hu Xia, Liang Lijuan, Xiao Zhenghui, Tan Lihong. (2019). The Clinical and Epidemiological Study of Children with Hand, Foot, and Mouth Disease in Hunan, China from 2013 to 2017. *Sci Rep*, 9(1), 11662. doi:10.1038/s41598-019-48259-1
3. Zhang Yan, Zhu Zhen, Yang Weizhong, *et al.* (2010). An emerging recombinant human enterovirus 71 responsible for the 2008 outbreak of hand foot and mouth disease in Fuyang city of China. *Virology*. 2010; 7:94. doi: 10.1186/1743-422X-7-94.
4. Yip Cyril C Y., Lau Susanna K P., Woo Patrick C Y., Yuen Kwok-Yung. (2013). Human enterovirus 71 epidemics: what's next? *Emerg Health Threats J*. 2013; 6:19780. doi: 10.3402/ehth.v6i0.19780.
5. Zhao Y Y, Jin H, Zhang X F, Wang B. (2015). Case-fatality of hand, foot and mouth disease associated with EV71: a systematic review and meta-analysis. *Epidemiol. Infect.* 143(14), 3094–102. doi:10.1017/S095026881500028X

6. Dang Dejian, Zhang Chao, Zhang Rongguang, *et al.*(2017). Involvement of inducible nitric oxide synthase and mitochondrial dysfunction in the pathogenesis of enterovirus 71 infection. *Oncotarget*, 8(46), 81014–81026. doi:10.18632/oncotarget. 21250
7. Chang Zhangmei, Wang Yan, Bian Liang *et al.* Enterovirus 71 antagonizes the antiviral activity of host STAT3 and IL-6R with partial dependence on virus-induced miR-124. *J Gen Virol*, 2017, 98: 3008–3025.
8. Wang Hui-Qiang, Hu Jin, Yan Hai-Yan, *et al.* (2017). Corydaline inhibits enterovirus 71 replication by regulating COX-2 expression. *J Asian Nat Prod Res*, 19(11), 1124–1133. doi:10.1080/10286020.2017.1386658
9. Tung Wei-Hsuan, Hsieh Hsi-Lung, Lee I-Ta, Yang Chuen-Mao. (2011). Enterovirus 71 modulates a COX-2/PGE2/cAMP-dependent viral replication in human neuroblastoma cells: role of the c-Src/EGFR/p42/p44 MAPK/CREB signaling pathway. *J Cell Biochem*, 112(2), 559–70. doi:10.1002/jcb.22946
10. Li Junru, Li Huifang, Yu Yu, *et al.*(2019). Via Mannan-binding lectin suppresses growth of hepatocellular carcinoma by regulating hepatic stellate cell activation the ERK/COX-2/PGE pathway. *Oncoimmunology*, 8(2), e1527650. doi:10.1080/2162402X.2018.1527650
11. Yan Guifang, Zhao Huakan, Zhang Qi, *et al.* (2018). A RIPK3-PGE Circuit Mediates Myeloid-Derived Suppressor Cell-Potentiated Colorectal Carcinogenesis. *Cancer Res.*, 78(19), 5586–5599. doi:10.1158/0008-5472.CAN-17-3962
12. Zhang Yanli, Xu Boyi, Luan Bin, *et al.* (2019). Myeloid-derived suppressor cells (MDSCs) and mechanistic target of rapamycin (mTOR) signaling pathway interact through inducible nitric oxide synthase (iNOS) and nitric oxide (NO) in asthma. *Am J Transl Res*, 11(9), 6170–6184.
13. Schmid Maximilian, Wege Anja K, Ritter Uwe. (2012). Characteristics of "Tip-DCs and MDSCs" and Their Potential Role in Leishmaniasis. *Front Microbiol*. 2012 Mar 12; 3:74. doi: 10.3389/fmicb.2012.00074. eCollection 2012.
14. Parker Katherine H., Beury Daniel W., Ostrand-Rosenberg Suzanne. (2015). Myeloid-Derived Suppressor Cells: Critical Cells Driving Immune Suppression in the Tumor Microenvironment. *Adv Cancer Res*. 2015; 128:95–139. doi: 10.1016/bs.acr.
15. Tanaka Tomoko, Fujita Mitsugu, Hasegawa Hiroshi, *et al.* (2017). Frequency of Myeloid-derived Suppressor Cells in the Peripheral Blood Reflects the Status of Tumor Recurrence. *Anticancer Res*, 37(7), 3863–3869. doi:10.21873/anticancer.11766
16. Domblides Charlotte, Lartigue Lydia, Faustin Benjamin (2018). Metabolic Stress in the Immune Function of T Cells, Macrophages and Dendritic Cells. *Cells*, 7(7):E68. doi:10.3390/cells7070068
17. Bergenfelz Caroline, Roxå Anna, Mehmeti Meliha, Leandersson Karin, Larsson Anna-Maria (2020). Clinical relevance of systemic monocytic-MDSCs in patients with metastatic breast cancer. *Cancer Immunol Immunother*, Epub ahead of print. doi:10.1007/s00262-019-02472-z
18. Telatin Valentina, Nicoli Francesco, Frasson Chiara, *et al* (2019). In Chronic Hepatitis C Infection, Myeloid-Derived Suppressor Cell Accumulation and T Cell Dysfunctions Revert Partially and Late

- After Successful Direct-Acting Antiviral Treatment. *Front Cell Infect Microbiol*, 9:190. doi:10.3389/fcimb.2019.00190.
19. Li Yiting, Zeng Yingfu, Zeng Guofen, *et al* (2019). The effects of direct-acting antiviral agents on the frequency of myeloid-derived suppressor cells and natural killer cells in patients with chronic hepatitis C. *J Med Virol*, 91(2): 278–286. doi:10.1002/jmv.25302
 20. Jayaraman Padmini, Parikh Falguni, Newton Jared M, *et al*. TGF- β 1 programmed myeloid-derived suppressor cells (MDSC) acquire immune-stimulating and tumor killing activity capable of rejecting established tumors in combination with radiotherapy. *Oncoimmunology*, 7(10), e1490853. doi:10.1080/2162402X.2018.1490853
 21. Khong Wei Xin, Yan Benedict, Yeo Huimin, *et al*. (2012). A non-mouse-adapted enterovirus 71 (EV71) strain exhibits neurotropism, causing neurological manifestations in a novel mouse model of EV71 infection. *J Virol*, 86(4), 2121–31. doi:10.1128/JVI.06103-11
 22. Wang Ya-Fang, Chou Chun-Ting, Lei Huan-Yao, *et al*.(2004). A mouse-adapted enterovirus 71 strain causes neurological disease in mice after oral infection. *J. Virol.*, 78(15), 7916–24. doi:10.1128/JVI.78.15.7916-7924.2004
 23. Wang Wei, Duo Jianying, Liu Jiangning, *et al*. (2011). A mouse muscle-adapted enterovirus 71 strain with increased virulence in mice. *Microbes Infect*, 13(10), 862–70. doi:10.1016/j.micinf.2011.04.004
 24. Su Lingkai, Xu Qingan, Zhang Ping, *et al* (2017). Phenotype and Function of Myeloid-Derived Suppressor Cells Induced by *Porphyromonas gingivalis* Infection. *Infect Immun*, 85(8): e00213-17. Doi: 10.1128 /IAI.00213 – 17.
 25. Khaled Yazan S, Ammori Basil J, Elkord Eyad.(2014). Increased levels of granulocytic myeloid-derived suppressor cells in peripheral blood and tumour tissue of pancreatic cancer patients. *J Immunol Res*, 879897. doi:10.1155/2014/879897.
 26. Lee Cho-Rong, Kwak Yewon, Yang Taewoo, *et al* (2016). Myeloid-Derived Suppressor Cells Are Controlled by Regulatory T Cells via TGF- β during Murine Colitis. *Cell Rep*, 17(12), 3219–3232. doi:10.1016/j.celrep.2016.11.062
 27. Xu Yujun, Xue Yaxian, Liu Xinghan, *et al*. (2019). Ferumoxylol Attenuates the Function of MDSCs to Ameliorate LPS-Induced Immunosuppression in Sepsis. *Nanoscale Res Lett*, 14(1), 379. doi:10.1186/s11671-019-3209-2
 28. John Vini, Kotze Leigh A, Ribechini Eliana, *et al*. (2019) Caveolin-1 Controls Vesicular TLR2 Expression, p38 Signaling and T Cell Suppression in BCG Infected Murine Monocytic Myeloid-Derived Suppressor Cells. *Front Immunol*, 10, 2826. doi:10.3389/fimmu.2019.02826
 29. Yan Guifang, Zhao Huakan, Zhang Qi, *et al*. (2018). A RIPK3-PGE Circuit Mediates Myeloid-Derived Suppressor Cell-Potentiated Colorectal Carcinogenesis. *Cancer Res.*, 78(19), 5586–5599. doi:10.1158/0008-5472.CAN-17-3962
 30. Pallett Laura J, Gill Upkar S, Quaglia Alberto, *et al*. (2015). Metabolic regulation of hepatitis B immunopathology by myeloid-derived suppressor cells. *Nat. Med*, 21(6), 591–600. doi:10.1038/nm.3856

31. Rodriguez Paulo C, Ernstoff Marc S, Hernandez Claudia, *et al.* (2009). Arginase I-producing myeloid-derived suppressor cells in renal cell carcinoma are a subpopulation of activated granulocytes. *Cancer Res*, 69(4), 1553–60. doi:10.1158/0008-5472.CAN-08-1921
32. Serafini Paolo, Mgebroff Stephanie, Noonan Kimberly, Borrello Ivan. (2008). Myeloid-derived suppressor cells promote cross-tolerance in B-cell lymphoma by expanding regulatory T cells. *Cancer Res*, 68(13), 5439–49. doi:10.1158/0008-5472.CAN-07-6621
33. Mizukoshi Eishiro, Yamashita Tatsuya, Arai Kuniaki, *et al.* (2016). Myeloid-derived suppressor cells correlate with patient outcomes in hepatic arterial infusion chemotherapy for hepatocellular carcinoma. *Cancer Immunol. Immunother.*, 65(6), 715–25. doi:10.1007/s00262-016-1837-2
34. Ríos-Ibarra Clara Patricia, Lozano-Sepulveda Sonia, Muñoz-Espinosa Linda, *et al.* (2014) Downregulation of inducible nitric oxide synthase (iNOS) expression is implicated in the antiviral activity of acetylsalicylic acid in HCV-expressing cells. *Arch. Virol.*, 159(12), 3321–8. doi:10.1007/s00705-014-2201-5
35. Tacke Robert S, Lee Hai-Chon, Goh Celeste, *et al.* (2012) Myeloid suppressor cells induced by hepatitis C virus suppress T-cell responses through the production of reactive oxygen species. *Hepatology*, 55(2), 343–53. doi:10.1002/hep.24700
36. Qi Fangfang, Zuo Zejie, Hu Saisai, *et al.* (2018) An enriched environment restores hepatitis B vaccination-mediated impairments in synaptic function through IFN- γ /Arginase1 signaling. *Brain Behav. Immun.*, 71, 116–132. doi:10.1016/j.bbi.2018.04.003
37. Karakasheva Tatiana A, Waldron Todd J, Eruslanov Evgeniy, *et al.* (2015). CD38-Expressing Myeloid-Derived Suppressor Cells Promote Tumor Growth in a Murine Model of Esophageal Cancer. *Cancer Res.*, 75(19), 4074–85. doi:10.1158/0008-5472.CAN-14-3639
38. Pang Xiaoli, Song Hongxiao, Zhang Qianqian, *et al.* (2016). Hepatitis C virus regulates the production of monocytic myeloid-derived suppressor cells from peripheral blood mononuclear cells through PI3K pathway and autocrine signaling. *Clin. Immunol.*, 164(undefined), 57–64. doi:10.1016/j.clim.2016.01.014
39. Sato Yusuke, Shimizu Kanako, Shinga Jun, *et al.*(2015). Characterization of the myeloid-derived suppressor cell subset regulated by NK cells in malignant lymphoma. *Oncoimmunology*, 4(3), e995541. doi:10.1080/2162402X.2014.995541
40. El-Emshaty Hoda Mohamed, Nasif Wesam Ahmad, Mohamed Ibrahim Eldsoky (2015). Serum Cytokine of IL-10 and IL-12 in Chronic Liver Disease: The Immune and Inflammatory Response. *Dis Markers*, 707254. doi:10.1155/2015/707254
41. Tobin Richard P, Jordan Kimberly R, Kapoor Puja, *et al* (2019). IL-6 and IL-8 Are Linked With Myeloid-Derived Suppressor Cell Accumulation and Correlate With Poor Clinical Outcomes in Melanoma Patients. *Front Oncol*, 9:1223.doi:10.3389/fonc. 2019.01223.
42. Zhifeng Chen, Ruiqin Li, Zhichao Xie, *et al* (2014). IL-6, IL-10 and IL-13 are associated with pathogenesis in children with Enterovirus 71 infection. *Int J Clin Exp Med*. 7(9):2718–23. eCollection 2014.

43. Draghiciu Oana, Lubbers Joyce, Nijman Hans W, Daemen Toos (2015). Myeloid derived suppressor cells-An overview of combat strategies to increase immunotherapy efficacy. *Oncoimmunology*, 4(1), e954829. doi:10.4161/21624011.2014.954829
44. Pinton Laura, Solito Samantha, Damuzzo Vera, *et al* (2016). Activated T cells sustain myeloid-derived suppressor cell-mediated immune suppression. *Oncotarget*, 7(2):1168–84. doi:10.18632/oncotarget.6662.

Tables

Table 1 is available in the Supplementary Files section.

Figures

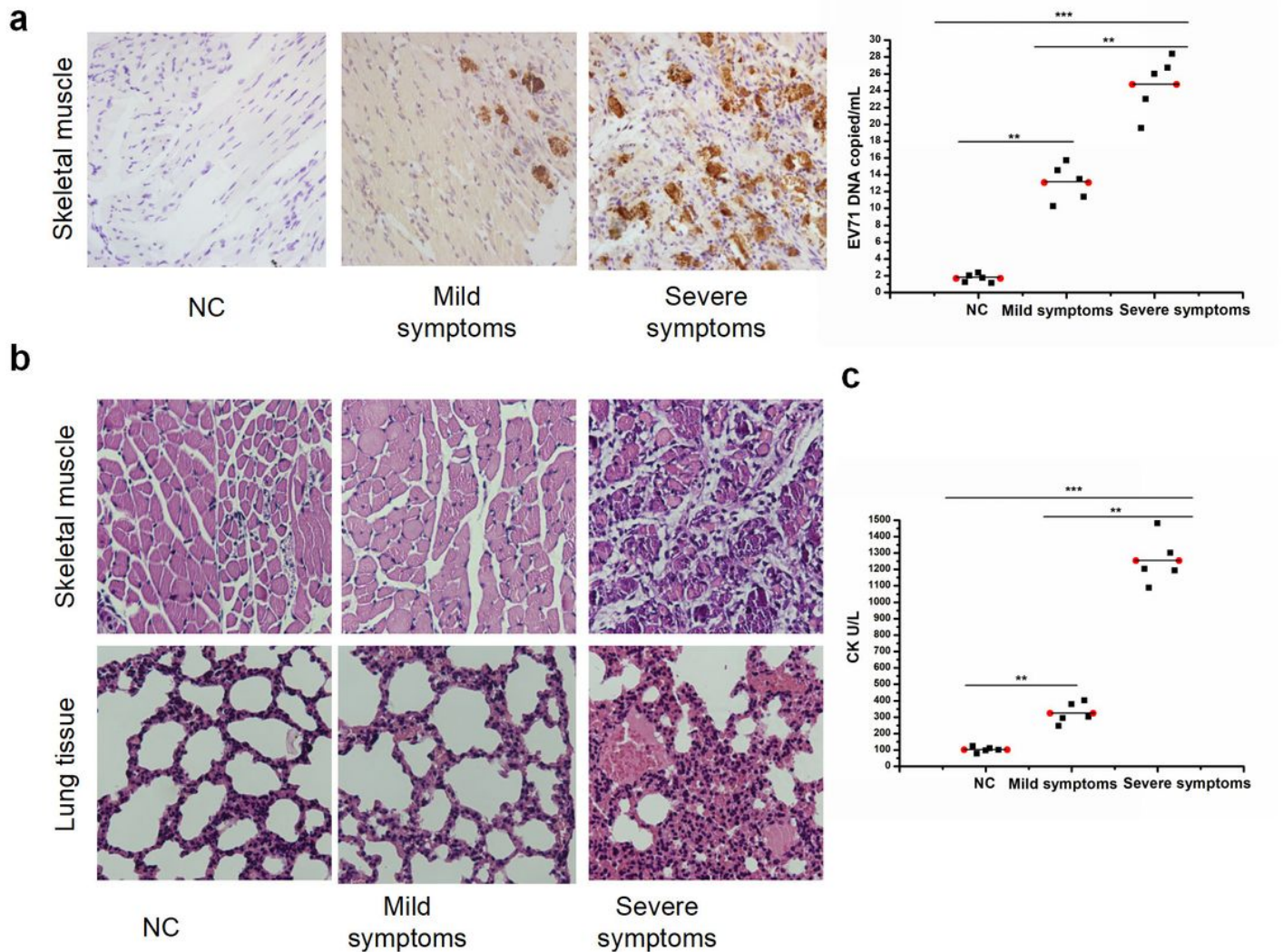


Figure 1

Establishment of the virus-infected mouse model (a) The qPCR analysis of EV71 replication and the immunohistochemistry analysis of VP1 protein expression in control mice and mice with either severe or mild symptoms (n=5); (b) The histopathological examination of skeleton muscle and lung tissue in different groups; (c) The CK (creatine kinase) level in the serum from these three groups were detected by ELISA (n=5). Data represent the mean \pm SEM. * $P < 0.05$, ** $P < 0.01$, and *** $P < 0.001$.

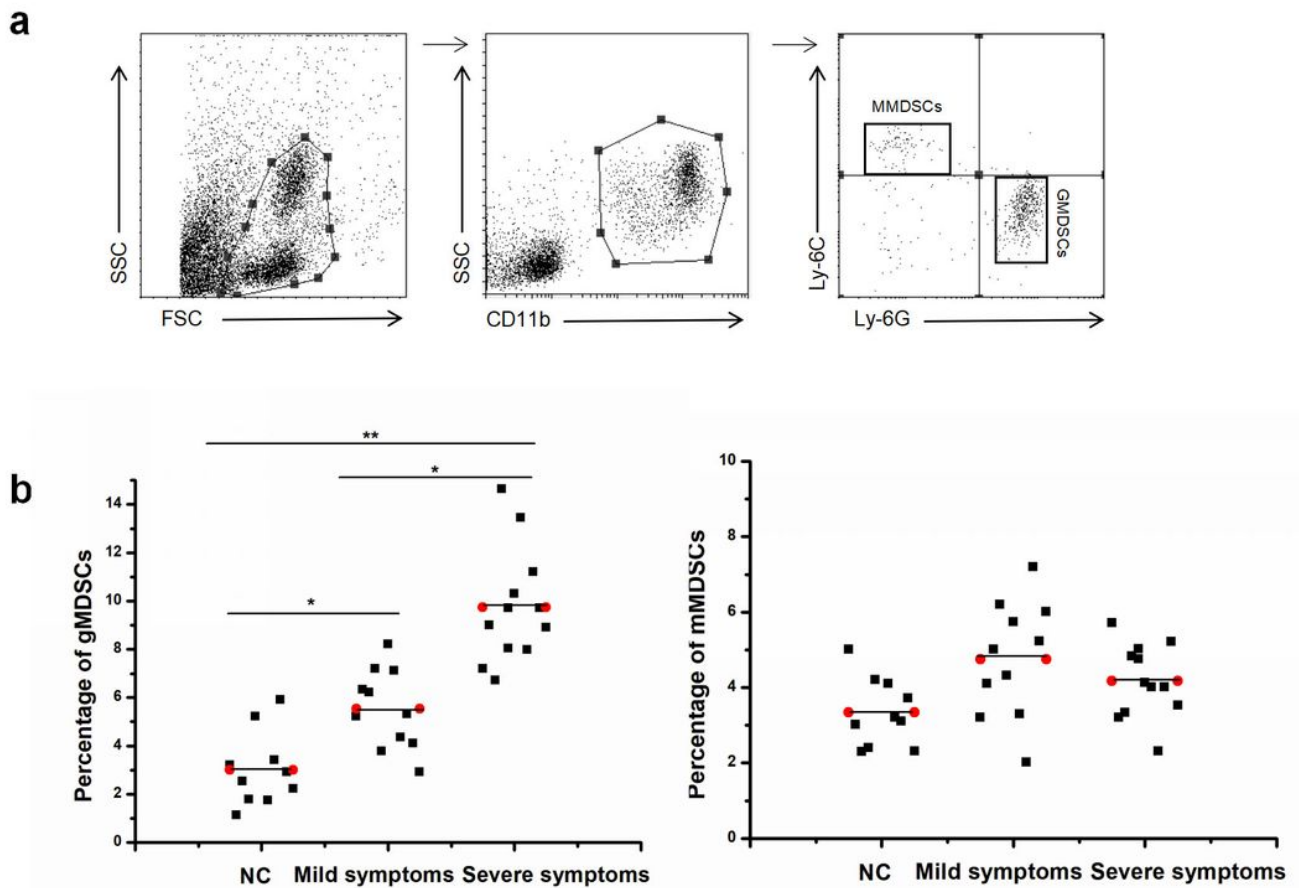


Figure 2

Correlations between MDSCs and EV71 infection in HFMD (a) Granulocytic myeloid-derived suppressor cells (gMDSCs) were defined as CD11b⁺ and Ly-6G⁺ cell populations; monocytic myeloid-derived suppressor cells (mMDSCs) were defined as CD11b⁺ and Ly-6C⁺ cells; (b) The percentages of gMDSCs and mMDSCs in the EV71-infected mice with severe symptoms (n=12), mild symptoms (n=11) and in negative mice (n=10). Data represent the mean \pm SEM. * $P < 0.05$, ** $P < 0.01$, and *** $P < 0.001$.

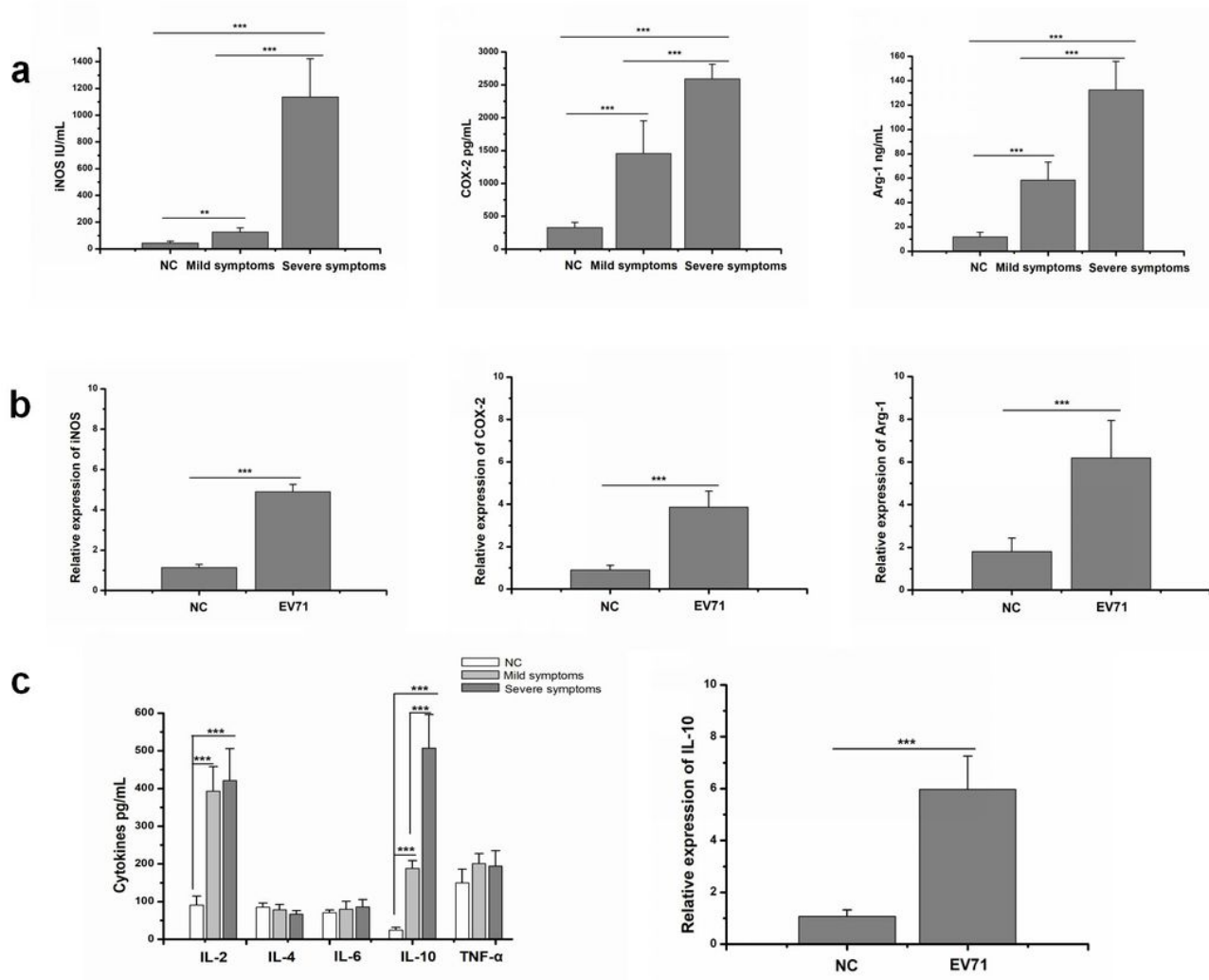


Figure 3

The expression of T-cell suppressors and cytokines in different groups (a) ELISA analyses of iNOS, COX-2 and Arg-1 in the negative control and EV71 infected mice with mild symptoms and severe symptoms (n=5). (b) In vitro qPCR analysis of iNOS, COX-2 and Arg-1 in the negative control and EV71 infection groups (n=4). (c) ELISA analyses of IL-2, IL-4, IL-6, IL-10 and TNF-α in the negative control and EV71 infected mice with mild symptoms and severe symptoms groups (n=5). In vitro qPCR analyses of IL-10 in the negative control and EV71 infection groups (n=4). Data represent the mean ± SEM. * $P < 0.05$, ** $P < 0.01$, and *** $P < 0.001$.

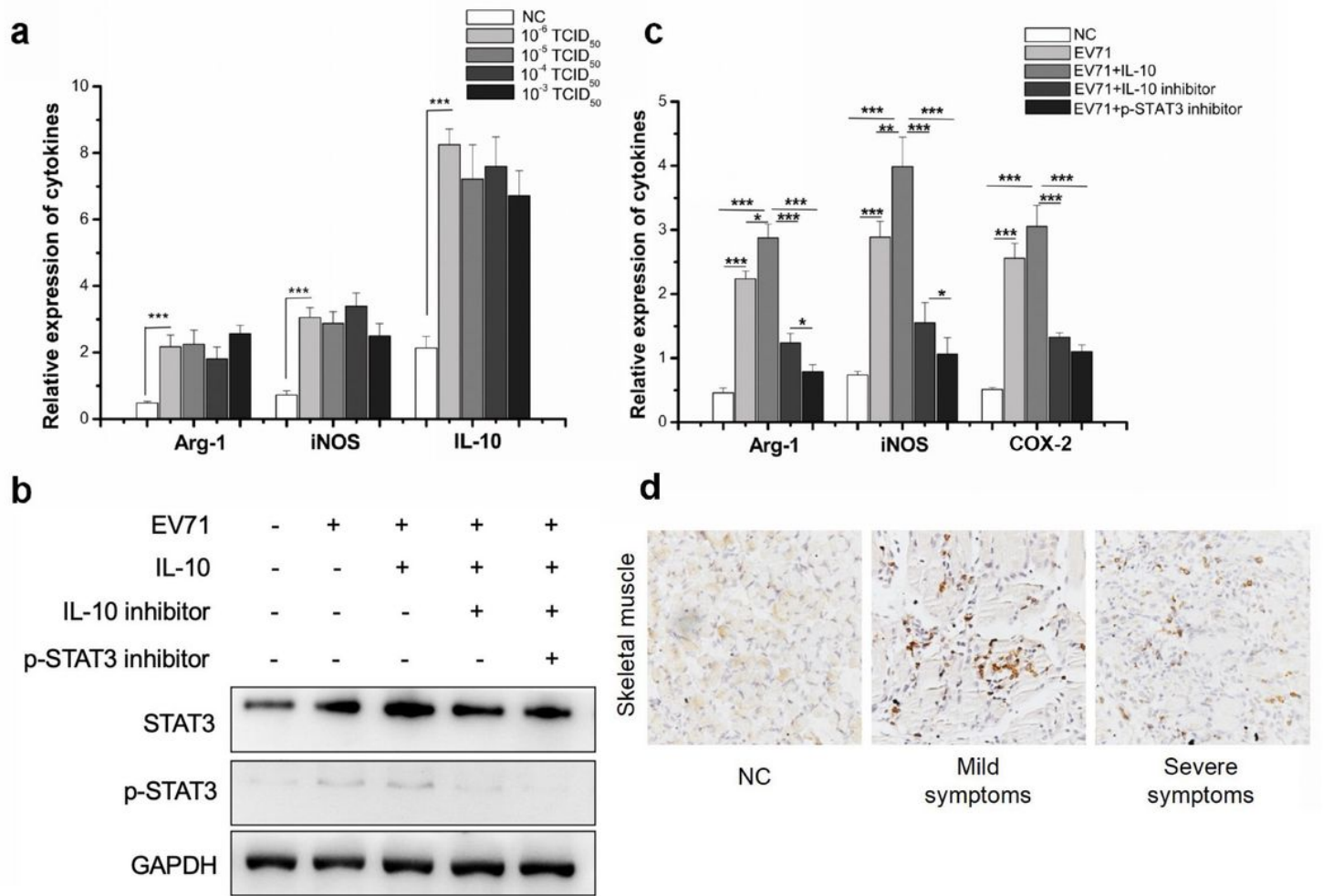


Figure 4

EV71 facilitates the inhibitory effects on T cells of gMDSCs through the IL-10/STAT3 signalling pathway

(a) In vitro qPCR analyses of iNOS, IL-10 and Arg-1 between the negative control group and the four EV71 infection groups with a concentration gradient from 10⁻³ TCID₅₀ to 10⁻⁶ TCID₅₀ (n=4). (b) The STAT3 phosphorylation in PBMCs treated with EV71, IL-10, IL-10 inhibitor, and/or p-STAT3 inhibitor for 12 hours evaluated by Western blot. The grouping of gels/blots cropped from different parts of the same gel. No high-contrast (overexposure) of blots was performed. (c) Arg-1, iNOS and COX-2 in PBMCs treated with EV71, IL-10, IL-10 inhibitor, and/or p-STAT3 inhibitor examined by qPCR (n=4). (d) The immunohistochemistry analysis of CD3 expression in control mice and mice with either severe or mild symptoms (n=5). Data represent the mean ± SEM. **P* < 0.05, ***P* < 0.01, and ****P* < 0.001.

Supplementary Files

This is a list of supplementary files associated with this preprint. Click to download.

- [Table1.pdf](#)